Reduced order modelling of gust responses.

Christopher Wales*, Ann Gaitonde †and Dorian Jones†

Aerospace Engineering, University of Bristol, Queen's Building, University Walk, Bristol, UK BS8 1TR

This paper describes two approaches to the construction of reduced order models (ROMs) from CFD to predict the gust response of airfoils and wings. The first is a linear ROM constructed using the eigensystem realisation algorithm (ERA) from pulse responses and the second approach modifies the linear ROM using steady state data to introduce some non-linearity into the ROM. Results are presented for the FFAST wing and the FFAST crank airfoil, where in the transonic regime for gusts of large amplitude the response exhibits non-linearity due to shock motion. This non-linearity is not captured well by linear ROMs, however the non-linear ROM shows better agreement with the full non-linear simulation results.

I. Introduction

A gust is an important phenomenon that affects an aircraft in flight. The loads on the aircraft can change very quickly causing a dynamic response that has significant implications for loads, control and passenger comfort. Simulating and estimating gust responses is therefore an important element of the design cycle as they often correspond to critical load cases.[1] In industry corrected linear doublet lattice methods are commonly used and comparison will be made to these techniques in this work. At low Mach numbers vertical gusts can induce large angles of attack that could result in a stall. At higher Mach number the induced changes in angle of attack due to the gust can have a significant impact on the strength and position of shocks. In both these examples the change in loads can therefore become non-linear due to the gust and any gust response model must therefore be able to accurately predict the loads for cases with flow non-linearities.

A move to CFD methods would permit high fidelity non-linear simulations of gust/aircraft encounters[2], however the computational costs would be much higher than the doublet lattice methods currently in use. The cost of simulations where a gust enters a domain and is introduced via the boundary conditions is

*Research Assistant, Aerospace Department
†Senior Lecturer, Aerospace Department

particularly high as a very fine mesh is needed throughout the computational domain in order to prevent the gust being dissipated numerically before it reaches the aircraft. Strategies to reduce the cost of CFD simulations for gusts therefore try to reduce the resolution of the mesh needed to convect the gust to/and past the aircraft. The two main approaches are local mesh refinement near the current gust location[3] and prescribed velocity methods. There have been a number of prescribed velocity methods described in literature. Some approaches (e.g. the Field Velocity Method) neglect terms in the Euler equations[4–6], whereas others (e.g. the Split Velocity Method) simply rearrange the Euler equations without simplification[7]. However whilst these approaches produce significant reductions in computational cost, the methods are still too computationally expensive compared to the doublet lattice methods for use in the design cycle. The creation of Reduced Order Models (ROMs) from CFD has been successfully applied to a range of other unsteady flow problems. If ROMs capable of predicting the non-linear forces on an aircraft during a gust encounter, can be created then they have the potential to greatly reduce computational costs.

In the fluid dynamics field ROMs can be created in either the time or frequency domain depending on the "training data" available from CFD simulation. Frequency domain approaches assume that the flow solution can be approximated as a sum of harmonics of one or more discrete frequencies. This assumption has been used within a number of ROM methods, with the two most common approaches being Eigenmode Summation (ES) and Proper Orthogonal Decomposition (POD)[8]. These methods have been applied to the Euler equations by for example Romanowski and Dowell[9] and Hall *et al*[10] respectively. Further development of a balanced POD has been achieved by Willcox and Peraire[11]. Such methods can also be applied in the time domain if appropriate training data can be identified. One alternative approach that has proved promising, identifies the discrete time pulse responses of the CFD code, which characterise all the solutions of the dynamically linear system[12–14]. Using the Eigensystem Realisation Algorithm (ERA)[15] the pulse responses can be used to generate a ROM. A major advantage of the ERA approach is that only minimal changes are required to any existing CFD code. This means that ERA and any developments from the basic method, can implemented using any CFD code within a short time to produce ROMs. This flexibility has led to the adoption of ERA as the basis for the development of a gust ROM in this work. Further detail on ERA, its relationship to POD and its application to control(including a methodology for projection of nonlinear dynamics or to retain parameters in the models) can be found in Ma *et al*[16].

In this paper two approaches for producing a ROM, for the gust response of airfoils and wings, from CFD data are investigated. The first of the two approaches used in this paper is a linear ROM constructed using the ERA method from a sharp edged gust response calculated using a prescribed velocity CFD method. The

second approach modifies the linear ROM to include information about the how the steady state gradient changes with increasing vertical velocity. This allows some non-linear data to be included in the model. The methods are tested on on both aerofoil and clean wing configurations, with the three dimensional results also compared to corrected doublet lattice.

II. Euler equations Rewritten Using Split Velocity Method

In order to generate ROMs using ERA, full order simulations of gust/airfoil interaction are required. As described above full order CFD simulations of gusts are expensive and in order to reduce the costs a split velocity method is employed here.[17] The Euler equations are rewritten using SVM by writing the Cartesian velocity components u, v, w as

$$u = \breve{u} + u_g; v = \breve{v} + v_g; w = \breve{w} + w_g \tag{1}$$

where u_g, v_g, w_g are the prescribed velocities describing the gust. The local values of these velocities are based on the gust profile that moves into the domain and its assumed progress at the free stream velocity. The energy is written as

$$E = \breve{E} + E_g \tag{2}$$

where

$$\begin{aligned} E &= \tfrac{p}{\rho(\gamma-1)} + \tfrac{1}{2}\left(u^2 + v^2 + w^2\right) \\ \breve{E} &= \tfrac{p}{\rho(\gamma-1)} + \tfrac{1}{2}\left(\breve{u}^2 + \breve{v}^2 + \breve{w}^2\right) \\ E_g &= (\breve{u}u_g + \breve{v}v_g + \breve{w}w_g) + \tfrac{1}{2}\left(u_g^2 + v_g^2 + w_g^2\right) \end{aligned} \tag{3}$$

The equations in integral form on a fixed mesh are given by

$$\frac{\mathrm{d}}{\mathrm{d}t}\int\int\int_{\Omega} \mathbf{W}\mathrm{d}x\mathrm{d}y\mathrm{d}z + \int\int_{\partial\Omega} (\mathbf{F}\mathrm{d}A_x + \mathbf{G}\mathrm{d}A_y + \mathbf{H}\mathrm{d}A_z) + \int\int\int_{\Omega} \mathbf{S}\mathrm{d}x\mathrm{d}y\mathrm{d}z = 0 \tag{4}$$

where

$$\begin{aligned} \mathbf{W} &= \left[\rho, \rho\breve{u}, \rho\breve{v}, \rho\breve{w}, \rho\breve{E}\right]^T \\ \mathbf{F} &= \left[\rho(\breve{u}+u_g), \rho\breve{u}(\breve{u}+u_g)+p, \rho\breve{v}(\breve{u}+u_g), \rho\breve{w}(\breve{u}+u_g), \rho\breve{E}(\breve{u}+u_g)+p\breve{u}\right]^T \\ \mathbf{G} &= \left[\rho(\breve{v}+v_g), \rho\breve{u}(\breve{v}+v_g), \rho\breve{v}(\breve{v}+v_g)+p, \rho\breve{w}(\breve{v}+v_g), \rho\breve{E}(\breve{v}+v_g)+p\breve{v}\right]^T \\ \mathbf{H} &= \left[\rho(\breve{w}+w_g), \rho\breve{u}(\breve{w}+w_g), \rho\breve{v}(\breve{w}+w_g), \rho\breve{w}(\breve{w}+w_g)+p, \rho\breve{E}(\breve{w}+w_g)+p\breve{w}\right]^T \\ \mathbf{S} &= [0, s_m(u_g), s_m(v_g), s_m(w_g), s_e(u_g, v_g, w_g)]^T \end{aligned} \tag{5}$$

Here the source terms are defined by

$$\begin{aligned} s_m(.) &= \rho\{\tfrac{\partial .}{\partial t} + (\breve{u} + u_g)\tfrac{\partial .}{\partial x} + (\breve{v} + v_g)\tfrac{\partial .}{\partial y} + (\breve{w} + w_g)\tfrac{\partial .}{\partial z}\} \\ s_e(u_g, v_g, w_g) &= \breve{u}s_m(u_g) + \breve{v}s_m(v_g) + \breve{w}s_m(w_g) + p\left(\tfrac{\partial u_g}{\partial x} + \tfrac{\partial v_g}{\partial y} + \tfrac{\partial w_g}{\partial z}\right) \end{aligned} \tag{6}$$

To minimise dissipation of the source terms, analytical derivatives are used inside the integrals, as the derivatives are only of the prescribed components that model the gust entering the domain. Preliminary studies indicated that these source terms are generally negligible except when there are large gradients in either the prescribed gust or the flow field (such as close to a body surface). This explains why the Field Velocity Method (FVM) works in many cases as it has similarities to SVM, but does not include the source terms.

It should be noted that no assumptions are made, nor any terms neglected. The equations have simply been rewritten in an alternative form. Further, the form of the equations is such that any CFD which has been written for a moving mesh can easily be run as an SVM code by

(a) setting grid velocities to minus the gust velocities, while keeping the mesh fixed

$$x_t = -u_g \quad y_t = -v_g \quad z_t = -w_g \tag{7}$$

(b) adding the source terms

The velocities and energy calculated in the moving grid code are then $\breve{u}$, $\breve{v}$, $\breve{w}$ and $\breve{E}$, however the pressures will be true pressures.

III. System reduction

The approach to generating a reduced order model adopted here is to consider the dynamic perturbation of force coefficients about a non-linear baseline(steady state) flow. The basic ERA approach assumes that the behaviour of the dynamic perturbation is approximately linear about the non-linear baseline(steady state) flow resulting initially in a linear ROM. This linear ROM will subsequently be corrected using non-linear steady state data to obtain a non-linear ROM.

A. Linear ROM using ERA

In this paper, only the case of a vertical gust will be considered. Hence $u_g = 0; w_g = 0$ for all time and v_g depends on the gust profile introduced to the domain and its progress, which is modelled as taking place at

the free stream velocity. Note that the gust profile is actually modified as it approaches the aircraft, but this is accounted for in the velocity components $\breve{u}, \breve{v}, \breve{w}$. The gust velocity profile that enters the domain can take any form. In system form, the equations can be represented as a single input system. The single input is taken as either the velocity of the gust at the edge of the domain where the gust first enters, or the velocity as the gust passes some fixed point within the domain before the presence of the gust can be detected in the responses. This input velocity is denoted by v_g^{in}. The linear dynamic behaviour of the perturbation in force coefficients about their mean values in response to a gust transit is therefore represented by a linear time-continuous state-space system

$$\begin{aligned} \dot{\mathbf{x}}(t) &= \mathbf{A}\mathbf{x}(t) + \mathbf{B}v_g^{in}(t) \\ \mathbf{y}(t) &= \mathbf{C}\mathbf{x}(t) + \mathbf{D}v_g^{in}(t) \end{aligned} \tag{8}$$

where $\mathbf{A}$,$\mathbf{B}$,$\mathbf{C}$ and $\mathbf{D}$ are the system matrices and the dot signifies differentiation with time. The state vector is $\mathbf{x}$ and the chosen output vector, $\mathbf{y}$, consists of the changes in lift and pitching moment coefficients from a steady state solution. Hence $\mathbf{y}$ is defined as

$$\mathbf{y} = \left[\hat{C}_l, \hat{C}_m\right]^T \tag{9}$$

In practice, in CFD the equations are actually solved in discrete-time space rather than in continuous-time space. Here a first order implicit finite difference scheme was used for the time derivative.

$$\begin{aligned} \frac{\tilde{\mathbf{x}}_k - \tilde{\mathbf{x}}_{k-1}}{\Delta t} &= \mathbf{A}\tilde{\mathbf{x}}_k + \mathbf{B}(\tilde{v}_g^{in})_k \\ \tilde{\mathbf{y}}_k &= \mathbf{C}\tilde{\mathbf{x}}_k + \mathbf{D}(\tilde{v}_g^{in})_k \end{aligned} \tag{10}$$

which on rearranging becomes

$$\begin{aligned} \tilde{\mathbf{x}}_k &= \tilde{\mathbf{A}}\tilde{\mathbf{x}}_{k-1} + \tilde{\mathbf{B}}(\tilde{v}_g^{in})_k \\ \tilde{\mathbf{y}}_k &= \tilde{\mathbf{C}}\tilde{\mathbf{x}}_k + \tilde{\mathbf{D}}(\tilde{v}_g^{in})_k \end{aligned} \tag{11}$$

where the discrete system matrices, identified by a tilde, are given by

$$\begin{aligned} \tilde{\mathbf{A}} &= (\mathbf{I} - \mathbf{A}\Delta t)^{-1} \\ \tilde{\mathbf{B}} &= (\mathbf{I} - \mathbf{A}\Delta t)^{-1}\mathbf{B}\Delta t \\ \tilde{\mathbf{C}} &= \mathbf{C} \\ \tilde{\mathbf{D}} &= \mathbf{D} \end{aligned} \tag{12}$$

These discrete system matrices (12) are a function of the time step used in the CFD simulation to put the

equations into dicrete-time form.

It will be seen in what follows, that using this first order scheme allows the discrete-time Markov parameters to be directly identified. These Markov parameters together with system input are all that are required to recreate the response of the discrete system (12) to any input. To simplify the process of obtaining a ROM of the discrete system, the system output is modified. As the output equation is known, matrix $\mathbf{D}$ is known, and so the $\tilde{\mathbf{D}}(\tilde{v}_g^{in})_k$ term can be subtracted from the equations to give a modified system output. The modified system is given by

$$\begin{aligned} \tilde{\mathbf{x}}_k &= \tilde{\mathbf{A}}\tilde{\mathbf{x}}_{k-1} + \tilde{\mathbf{B}}(\tilde{v}_g^{in})_k \\ \tilde{\mathbf{y}}_k^m &= \tilde{\mathbf{y}}_k - \tilde{\mathbf{D}}(\tilde{v}_g^{in})_k = \tilde{\mathbf{C}}\tilde{\mathbf{x}}_k \end{aligned} \tag{13}$$

If the initial system is undisturbed ($\tilde{\mathbf{x}}_{-1} = 0$) then the forced response of the modified system is given by

$$\tilde{\mathbf{y}}_l^m = [\mathbf{H}_l, \mathbf{H}_{l-1}, \ldots, \mathbf{H}_2, \mathbf{H}_1, \mathbf{H}_0] \begin{bmatrix} (\tilde{v}_g^{in})_0 \\ (\tilde{v}_g^{in})_1 \\ \vdots \\ (\tilde{v}_g^{in})_{l-2} \\ (\tilde{v}_g^{in})_{l-1} \\ (\tilde{v}_g^{in})_l \end{bmatrix} \tag{14}$$

where the following sequence $\mathbf{H}_k, k = 0, \infty$

$$\{\mathbf{H}_0, \mathbf{H}_1, \ldots, \mathbf{H}_3, \ldots, \mathbf{H}_k, \ldots\} = \{\tilde{\mathbf{C}}\tilde{\mathbf{B}}, \tilde{\mathbf{C}}\tilde{\mathbf{A}}\tilde{\mathbf{B}}, \ldots, \tilde{\mathbf{C}}\tilde{\mathbf{A}}^k\tilde{\mathbf{B}}, \ldots\} \tag{15}$$

is called the Markov, impulse-response or weighting sequence of the system and $\mathbf{H}_0, \mathbf{H}_1, \ldots$ are the Markov parameters. Thus any two systems with identical Markov sequences have identical forced responses for the same input. Note that for a system of rank n the sequence $\mathbf{H}_k; k = 0; 2n$ defines the forced response exactly.

If a value for each Markov parameter can be extracted from responses of the system, then the size of the system matrices $\tilde{\mathbf{A}}$, $\tilde{\mathbf{B}}$ and $\tilde{\mathbf{C}}$ can be reduced using the Eigensystem Realization Algorithm.[15] In ERA, the Markov parameters are first used to construct a Hankel matrix. For a large system such as an Euler system, the Hankel matrix required to fully define the linear system would be prohibitively large and ERA would offer little or no advantage over solving the full Euler equations. In practice for certain large systems, it is possible to identify the dominant behaviour in the training data using a relatively small truncated Hankel

matrix. The Hankel matrix in this case is the $r \times s$ block matrix given by

$$\mathbf{H}_{rs}(k) = \begin{bmatrix} \mathbf{H}_k & \mathbf{H}_{k+1} & \dots & \mathbf{H}_{k+s-1} \\ \mathbf{H}_{k+1} & \mathbf{H}_{k+2} & \dots & \mathbf{H}_{k+s} \\ \vdots & \vdots & \ddots & \vdots \\ \mathbf{H}_{k+r-1} & \mathbf{H}_{k+r} & \dots & \mathbf{H}_{k+s+r-2} \end{bmatrix} \tag{16}$$

For a general multiple input multiple output system, with m inputs and p outputs, each Markov parameter is a $p \times m$ matrix and the Hankel matrix is of size $rp \times sm$. Here $m = 1$ and $p = 2$.

The next step in the ERA process is to obtain a singular-value decomposition (SVD) of the Hankel matrix $\mathbf{H}_{rs}(0)$, which is given by

$$\mathbf{H}_{rs}(0) = \mathbf{U}\mathbf{\Sigma}\mathbf{V}^T \tag{17}$$

where Σ is a diagonal matrix whose entries are the singular values. The elements of $\mathbf{\Sigma}$ are ordered so the largest singular-values are first. The rank of the ROM, r, is determined by either taking a user prescribed number of the largest singular values or taking all elements of Σ larger than some desired size. The Hankel matrix is then partitioned as

$$\mathbf{H}_{rs}(0) = \begin{bmatrix} \mathbf{U}_r & \mathbf{U}_0 \end{bmatrix} \begin{bmatrix} \mathbf{\Sigma}_r & 0 \\ 0 & \mathbf{\Sigma}_0 \end{bmatrix} \begin{bmatrix} \mathbf{V}_r \\ \mathbf{V}_0 \end{bmatrix}^T \tag{18}$$

and matrix $\mathbf{H}_{rs}(0)$ can be approximated by

$$\mathbf{H}_{rs}(0) = \mathbf{U}_r\mathbf{\Sigma}_r\mathbf{V}_r^T \tag{19}$$

There are several possible realisations and in this work a balanced realisation[15] is used, given by

$$\begin{aligned} \tilde{\mathbf{A}}_r &= \mathbf{\Sigma}_r^{-1/2}\mathbf{U}_r^T\mathbf{H}_{rs}(1)\mathbf{V}_r\mathbf{\Sigma}_r^{-1/2} \\ \tilde{\mathbf{B}}_r &= \mathbf{\Sigma}_r^{1/2}\mathbf{V}_r^T\mathbf{E}_m \\ \tilde{\mathbf{C}}_r &= \mathbf{E}_p^T\mathbf{U}_r\mathbf{\Sigma}_r^{1/2} \end{aligned} \tag{20}$$

where $\tilde{\mathbf{A}}_r$, $\tilde{\mathbf{B}}_r$ and $\tilde{\mathbf{C}}_r$ are the reduced order discrete system matrices. $\mathbf{E}_p^T = [\mathbf{I}_p, 0_p, 0_p, \dots, 0_p]$ is of size $p \times rp$ and $\mathbf{E}_m^T = [\mathbf{I}_m, 0_m, 0_m, \dots, 0_m]$ is of size $m \times nm$. $\mathbf{I}_p$ and $\mathbf{I}_m$ are the $p \times p$ and $m \times m$ identity matrices respectively.

B. Extraction of the Markov parameters from Euler simulations

The ERA approach described above assumes a dynamically linear system, relative to a non-linear mean. Hence in order to extract the Markov parameters it is necessary to be able to obtain a linear response from the Euler equations. This can be generated directly from a dynamically linearised Euler code[14] or alternatively can be approximately identified from the non-linear CFD code using Volterra theory[13]. In the latter case, for weakly non-linear systems the solution can be represented by a truncated Volterra series for small inputs. If the system may be approximated by a second order Volterra series, then using the notation of Silva[13], the first order kernel of the system, h_1 can be found from

$$h_1 = 2y_1 - \frac{1}{2}y_{11} \tag{21}$$

where y_1 represents the response of the non-linear system to an input and y_{11} represents the response to an equivalent input of twice the amplitude. If the non-linear system exhibits approximately linear behaviour to small inputs, then it can be assumed that the non-linear first order kernel is that of an approximating linear system. Thus the linear responses can be found from two responses of the non-linear CFD code. A comparison of the linear responses obtained using these approaches for pulse inputs can be found in Gaitonde and Jones[18].

Now the Markov parameters can be identified directly from the linear responses to a pulse input *i.e.* $(\tilde{v}_g^{in})_0 = 1$ and $(\tilde{v}_g^{in})_k = 0$ for $k > 0$. However, this was found not to be a good approach. The size of the effective pulse, which depends on the time step, relative to the mesh cells in the far field can mean that the change in vertical velocity may not impact on any cell centre, see Figure 1a. Therefore the pulse responses were obtained indirectly by differentiating a linear sharp edge gust response, using finite differences, see Figure 1b. The linear sharp edge gust response is generated using equation (21) from two non-linear responses to two sharp edged gusts of different amplitudes. In 2D the simulations have been performed using an in-house implementation of Jameson's cell-centred finite volume scheme and in 3D were performed using the DLR Tau CFD code[19,20]. These codes permit moving meshes and hence can easily be modified to incorporate SVM with only the addition of the source terms, that can be evaluated analytically for the step of size Δ shown in Figure 1[21].

C. Including steady state data

As described in the previous section the linear pulse response is extracted from the derivative of step responses. These linear pulse responses yield the Markov parameters and hence can be used in ERA to obtain

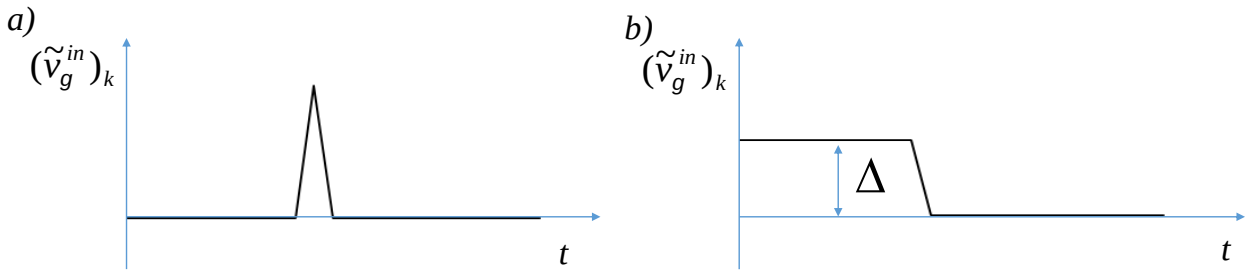

Figure 1. (a) Pulse input and (b) Step input

a linear gust ROM

$$\begin{aligned} \tilde{\mathbf{x}}_k^r &= \tilde{\mathbf{A}}_r \tilde{\mathbf{x}}_{k-1}^r + \tilde{\mathbf{B}}_r (\tilde{v}_g^{in})_k \\ \tilde{\mathbf{y}}_k &= \tilde{\mathbf{C}}_r \tilde{\mathbf{x}}_k^r \end{aligned} \tag{22}$$

where $\tilde{\mathbf{x}}^r$ is the reduced state space vector.

Non-linear effects are introduced through the use of non-linear steady-state data for the airfoil at various angles of attack. This corrected non-linear ROM is given by

$$\begin{aligned} \tilde{\mathbf{x}}_k^r &= \tilde{\mathbf{A}}_r \tilde{\mathbf{x}}_{k-1}^r + \tilde{\mathbf{B}}_r (\tilde{v}_g^{in})_k \\ \tilde{\mathbf{y}}_k &= \tilde{\mathbf{S}}[(\tilde{v}_g^{in})_k] \tilde{\mathbf{C}}_r \tilde{\mathbf{x}}_k^r \end{aligned} \tag{23}$$

where the scaling matrix $\tilde{\mathbf{S}}$ is calculated using the steady states for an equivalent change in angle of attack based on the gust velocity, given by

$$\tilde{\mathbf{S}}[(\tilde{v}_g^{in})_k] = \Delta C_f(\tilde{v}_g^{in})_k|_{CFD} / \Delta C_f(\tilde{v}_g^{in})_k|_{Linear} \tag{24}$$

IV. Test cases

The approaches outlined earlier are applied to the identification of a ROM for the response, of both the FFAST crank airfoil and the FFAST wing[22], to a gust. All the gusts investigated are 1-cosine vertical gusts and are defined by

$$v_g^{in} = \left\{ \begin{array}{lll} 0, & x < x' - l_g, & x > x' \\ \frac{v_{g_{max}}}{2} \left[1 - cos \frac{2\pi(x')}{l_g} \right], & x' \geq x \geq x' - l_g & \end{array} \right\}. \tag{25}$$

where l_g is the gust length, $v_{g_{max}}$ is the gust amplitude and x' is the leading edge position of the gust.

Four different length gusts with varying amplitudes were tested. The maximum gust velocity is a function of

the gust length, the four cases are summarised in Table 1. The free stream velocity is $250m/s$ at standard sea level conditions giving a Mach number of 0.735 and the airfoil and wing are both at zero degrees incidence.

Case	Gust length (m)	Gust magnitude (m/s)	Equivalent angle of attack change (deg)
1	125	15.61	3.57
2	500	19.69	4.50
3	875	21.60	4.94
4	1250	22.92	5.24

Table 1. Parameter values used for gust profiles in the test cases.

The wing geometry for the 3D test cases is the FFAST wing shown in Figure 2 and the airfoil geometry used for the 2D test cases is the crank section of the FFAST wing shown in Figure 3.

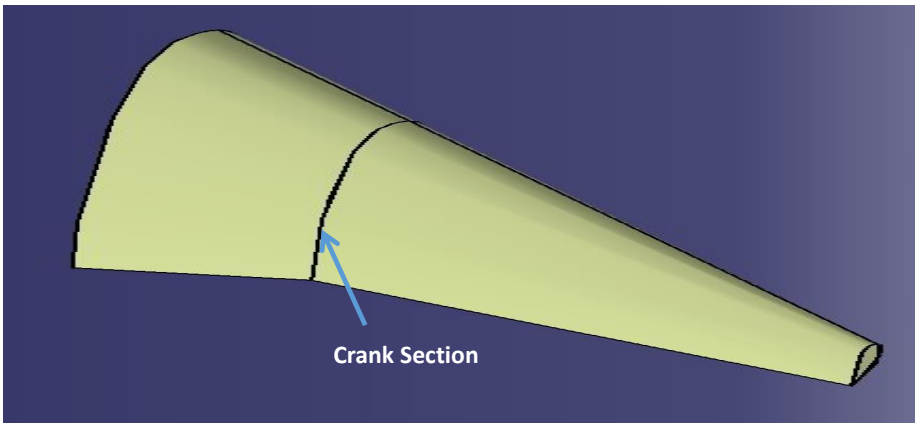

Figure 2. FFAST wing

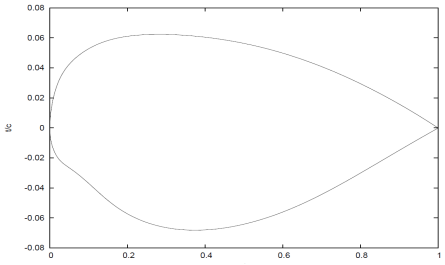

Figure 3. FFAST crank airfoil

V. 2D Results for the FFAST Crank airfoil

A. Rigid body motion

The linear component of the response to a sharp edge gust passing over the airfoil is shown in Figure 4. The lift and moment(about structural axis which is at 0.31 chord) coefficients have a long transient time in

comparison to the time the gust takes to pass over the airfoil, hence 750 Markov parameters were used to construct rank 30 linear ROMs and ROMs corrected using steady state data.

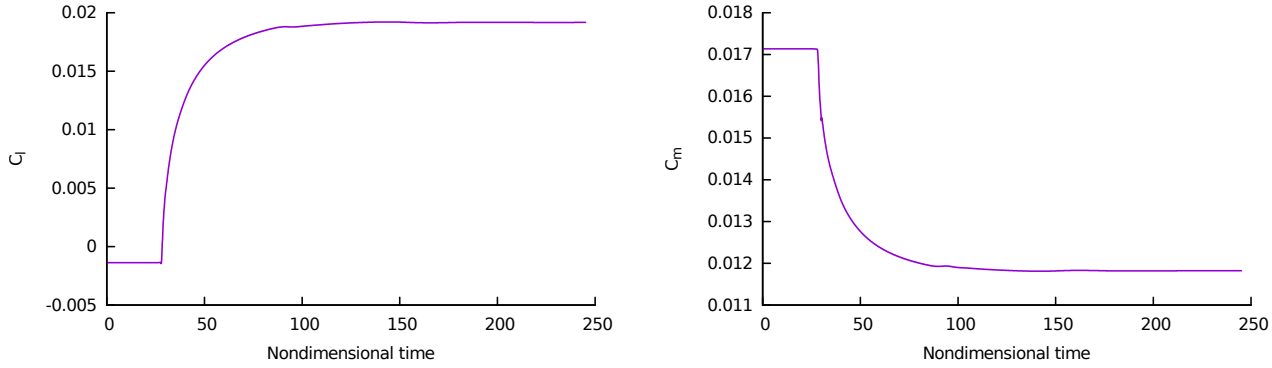

Figure 4. Lift and moment coefficient histories for a sharp edged gust at M=0.735

The lift and moment coefficient responses from linear and corrected ROMs for the four gust length test cases are compared to the full Euler responses simulated using the SVM approach[17] in Figures 5 to 8.

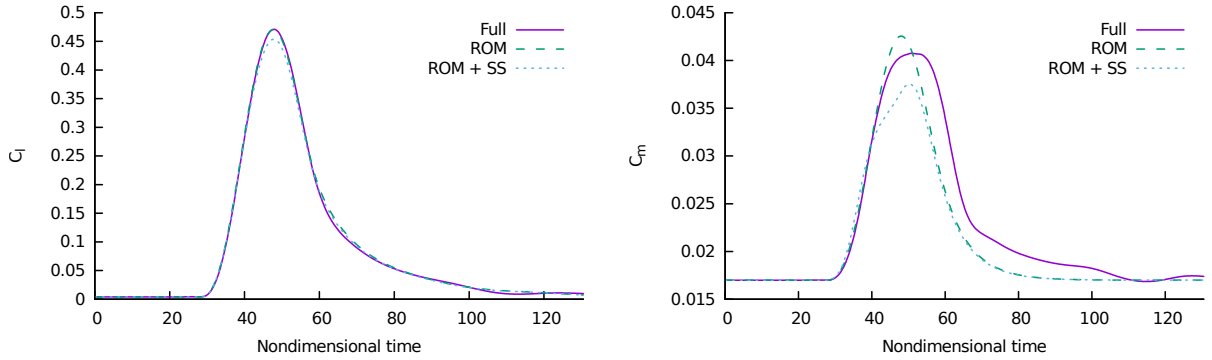

(a) C_l (b) C_m

Figure 5. Lift and moment coefficient histories for gust profile 1 at M=0.735

Whilst the linear ROM gives results that are close to full order CFD at the shortest gust length (Figure 5), for longer gust lengths it overpredicts the peak lift coefficient and underpredicts the peak magnitude of the moment coefficient. The non-linear ROM gives better predictions compared to the full order CFD except at the very shortest gust length (Figures 6 to 8). For this airfoil at zero degrees and Mach 0.735 there is a large shock motion during the gust transient, as shown for example in Figure 9 for gust 4. The effect of gust speed (which determines gust length) on the steady state moment used for correcting the linear ROM is shown in Figure 10, where a change in gradient as the speed increases is observed. This large shock motion and non-linearity in the coefficients at higher gust speeds is the cause of the deficiencies in the linear ROM. The linear method is better for the shorter gusts because the gust is not long enough for the shock to move as far and the correction applied is too large. It should be noted that for the lift both methods show a slightly

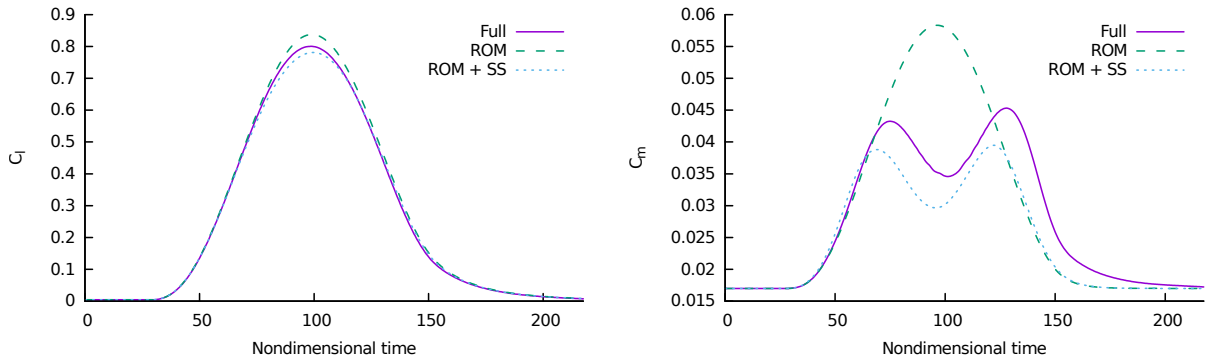

(a) C_l (b) C_m

Figure 6. Lift and moment coefficient histories for gust profile 2 at M=0.735

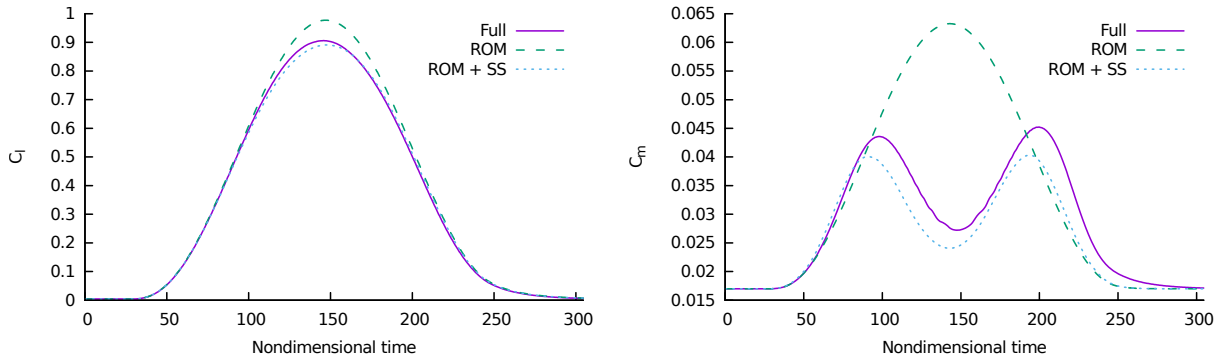

(a) C_l (b) C_m

Figure 7. Lift and moment coefficient histories for gust profile 3 at M=0.735

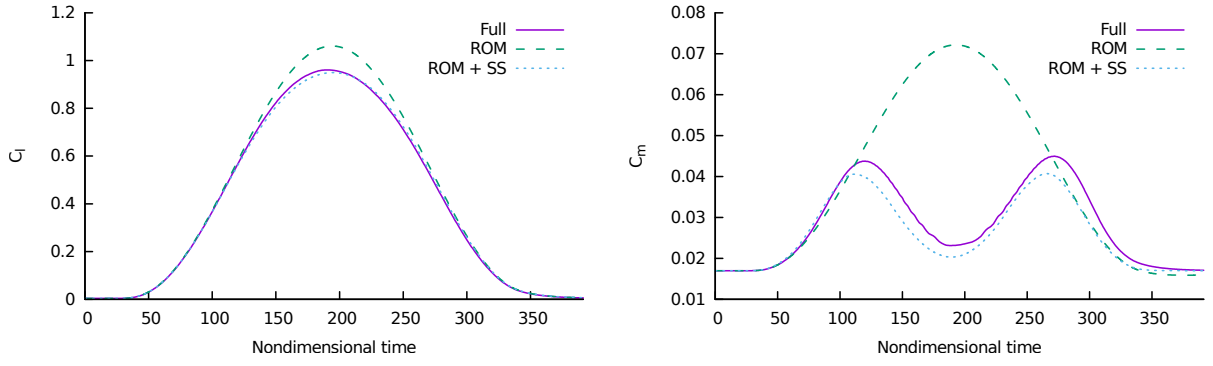

(a) C_l (b) C_m

Figure 8. Lift and moment coefficient histories for gust profile 4 at M=0.735

slower return to the mean flow solution then the full gust response, but a quicker return to the mean for the pitching moment.

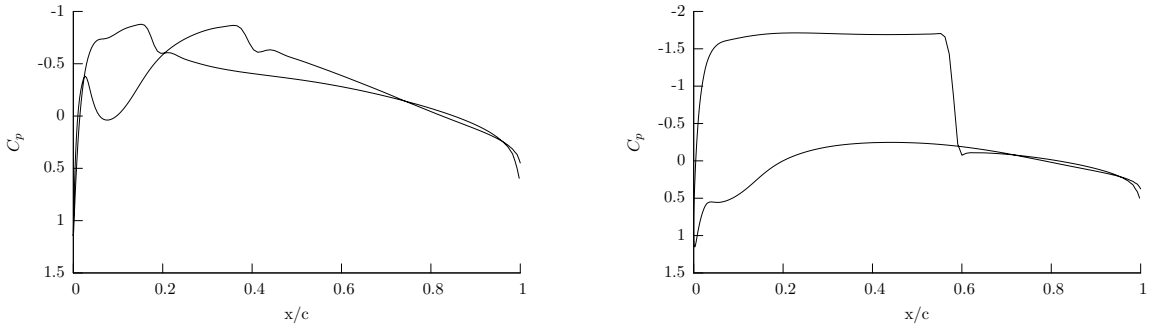

(a) C_l (b) C_m

Figure 9. Surface pressure coefficients around FFAST crank airfoil before gust and at peak moment magnitude for gust profile 4

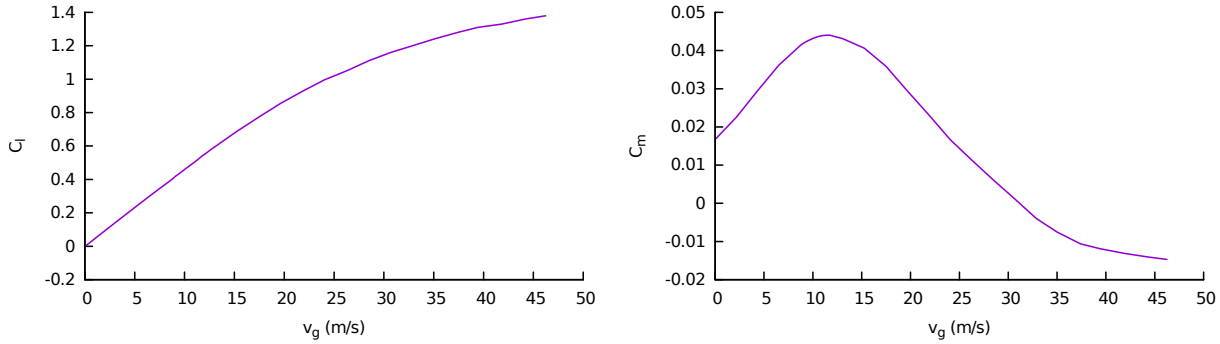

(a) C_l (b) C_m

Figure 10. Steady state lift and moment coefficient with gust velocity

B. Aeroelastic motion

The prediction of the aeroelastic gust response using ROMs is then demonstrated using a two-degree of freedom system model of the airfoil structure, with vertical heave translation and rotational pitch motion as shown in Figure 11. If it is assumed that there is no structural damping and the system has linear stiffness. The general equations of motions are

$$\begin{aligned} m\ddot{h} &+ mbx_\theta\ddot{\theta} &+ m\omega_h^2 h &= -L \\ mbx_\theta\ddot{h} &+ I_\theta\ddot{\theta} &+ I_\theta\omega_\theta\theta &= M_{ea} \end{aligned} \tag{26}$$

where the moment is given about the elastic axis which is at 0.31 x/c. The structural model parameters are given in Table 2 and x_θ is the position of the c.g. aft of the elastic axis.

The aerodynamic force response model is made up of two components: the first is the change in aerodynamic

Mass	$41240kg$	I_θ	$530100kgm^2$
K_h	$6.8 \times 10^6 N/m$	K_θ	$9.0 \times 10^7 N/m$
ω_h	$12.8409rad/s$	ω_θ	$13.0299rad/s$
x_θ	$-0.3882m$	b	$4.04m$
ρ_{air}	$1.225kg/m^3$		

Table 2. Structural model parameters

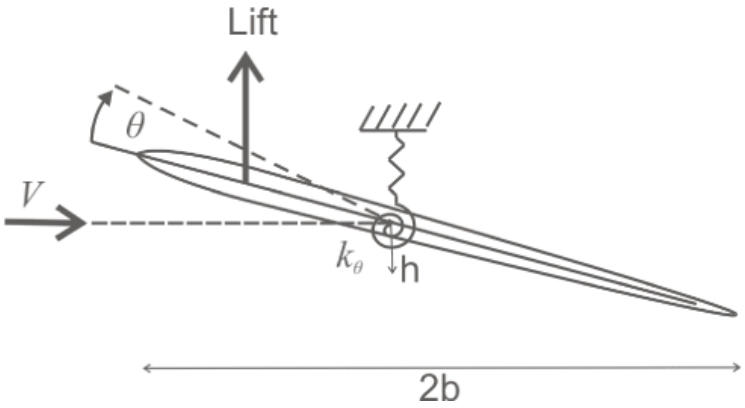

Figure 11. 2 DOF aeroelastic model

forces due to the airfoil motion and is modelled with a linear state space ROM, constructed using the system pulse responses and a restarted ERA approach[23]; the second component is the change in the aerodynamic forces due to the gust and this is calculated using either the linear ROM or the non-linear corrected ROM described above.

The two aerodynamic ROMs are combined and coupled with the structural model to calculate the aeroelastic responses to the same four gusts given in Table 1. The unsteady lift and pitching moment coefficients as well as the heave displacement and pitch angle are shown in Figures 12 to 15. The pitching moment coefficients are given about the structural axis which is at 0.31 chord.

For the shortest gust, shown in Figure 12 both ROMs predict the displacements and lift coefficient well. Both methods are less accurate near the peak moment value, with the linear ROM being slightly better. This is similar to the rigid responses seen previously in 5. For the longer gusts, the non-linear ROM outperforms the linear ROM which does not capture the "double peak" seen in the full order moment and pitch responses. Further the error in peak lift and heave displacement predicted by the linear ROM increases as the gust length increases, whereas the non-linear ROM continues to give good predictions. The structural responses once the gust has gone past the airfoil are in reasonable agreement for amplitude and frequency for both ROMs except for case 3, see Figure 14, where the ROMs predict a larger amplitude oscillation.

VI. 3D Results for the FFAST Wing in Rigid Body Motion

The ROM methods have also been applied in 3D. Calculations of the lift and moment responses of the FFAST wing for the gusts in Table 1 are shown in figures 16 to 19 for a linear ROM of size 40 created using a Hankel matrix of size 500. Again the pitching moment coefficients are given about the structural axis which is at 0.31 mean aerodynamic chord. The results are compared to the full CFD and uncorrected DLM calculated using NASTRAN. The linear ROM shows good agreement with the CFD for the lift response for all gust lengths while the DLM consistently under predicts the lift. However for the pitching moment the linear ROM and DLM over predict the change in pitching moment. This is because as the gust passes the shock moves leading to non-linearity in the moment coefficients. This can be seen by looking at the steady state pitching moment against equivalent gust speed in Figure 20, which shows a change in gradient as the vertical speed increases.

The DLM can be corrected so that the lift and moment curve slopes are matched to the CFD data. This is done using the W_{kk} matrix[24] in NASTRAN. Here the DLM is corrected to match the linear behaviour, upto gusts of 5m/s. The lift and moment responses for the corrected DLM (labelled DLM SS0) are also shown in

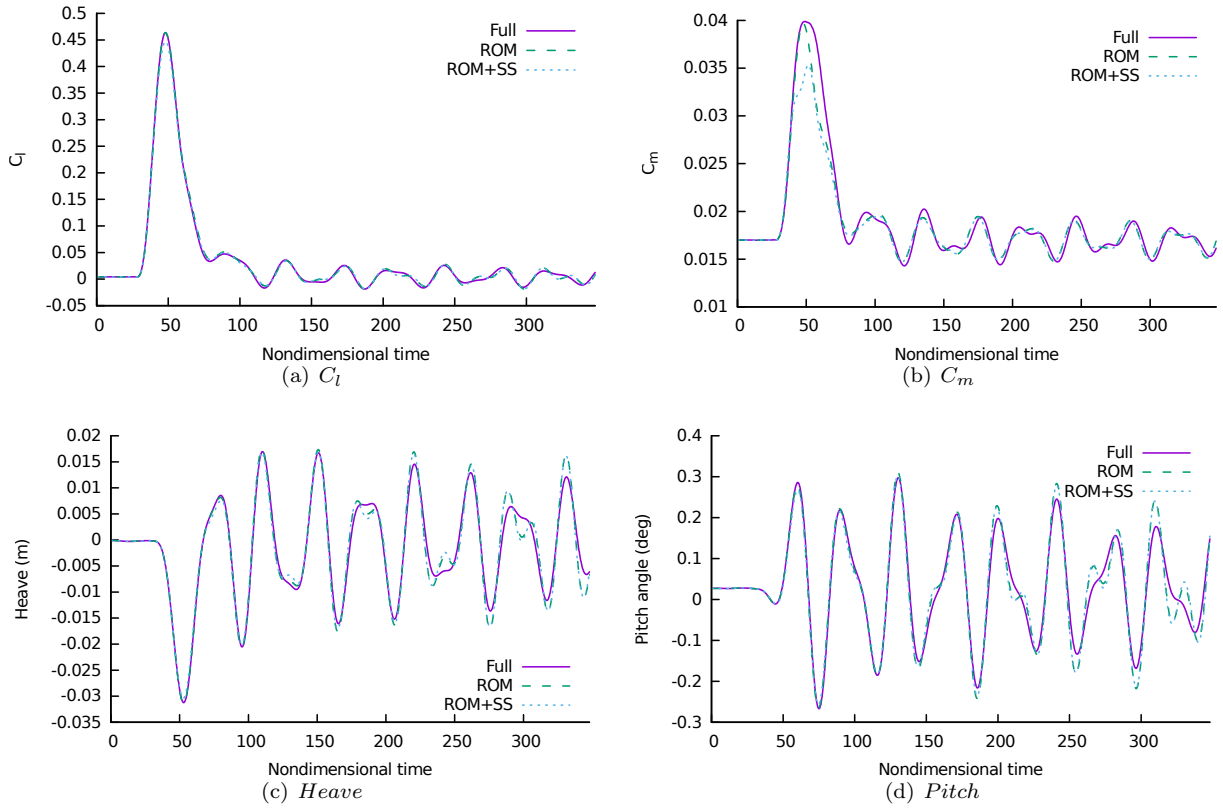

(a) C_l (b) C_m

(c) $Heave$ (d) $Pitch$

Figure 12. Aeroelastic response of crank airfoil to gust profile 1

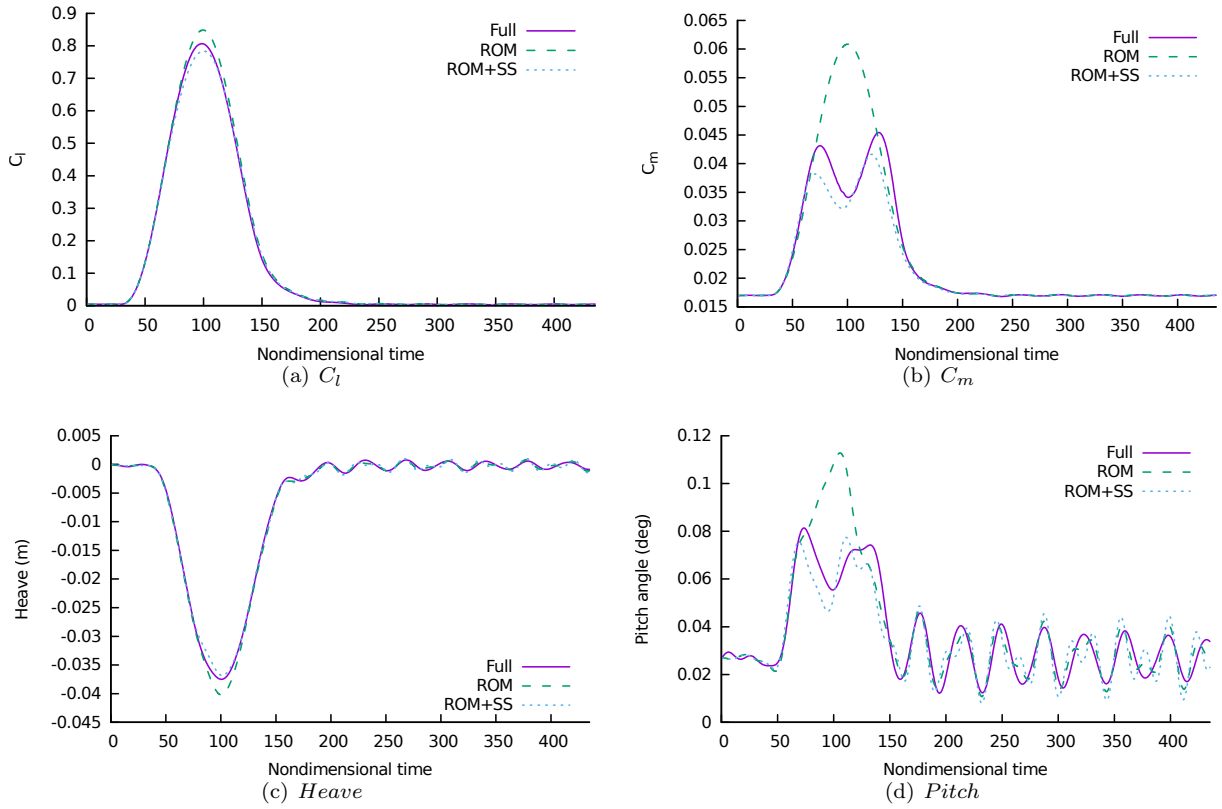

(a) C_l (b) C_m

(c) *Heave* (d) *Pitch*

Figure 13. Aeroelastic response of crank airfoil to gust profile 2

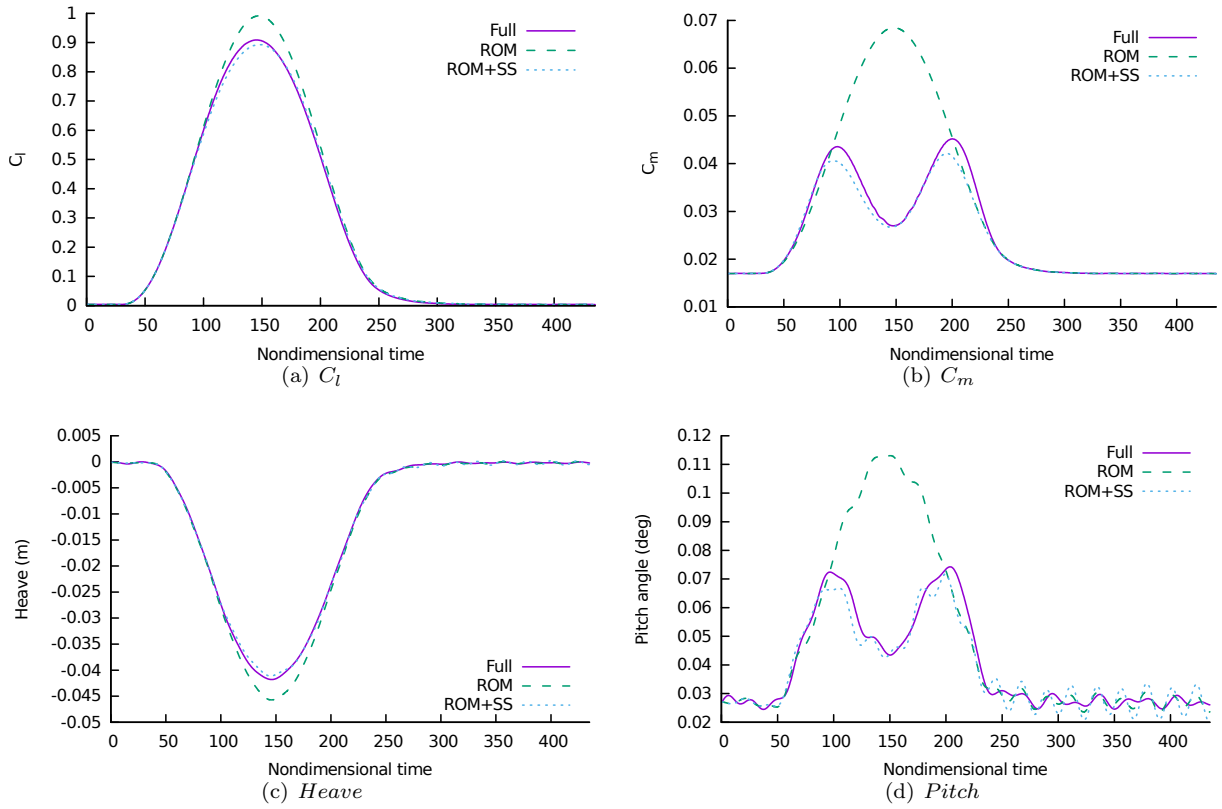

(a) C_l (b) C_m

(c) $Heave$ (d) $Pitch$

Figure 14. Aeroelastic response of crank airfoil to gust profile 3

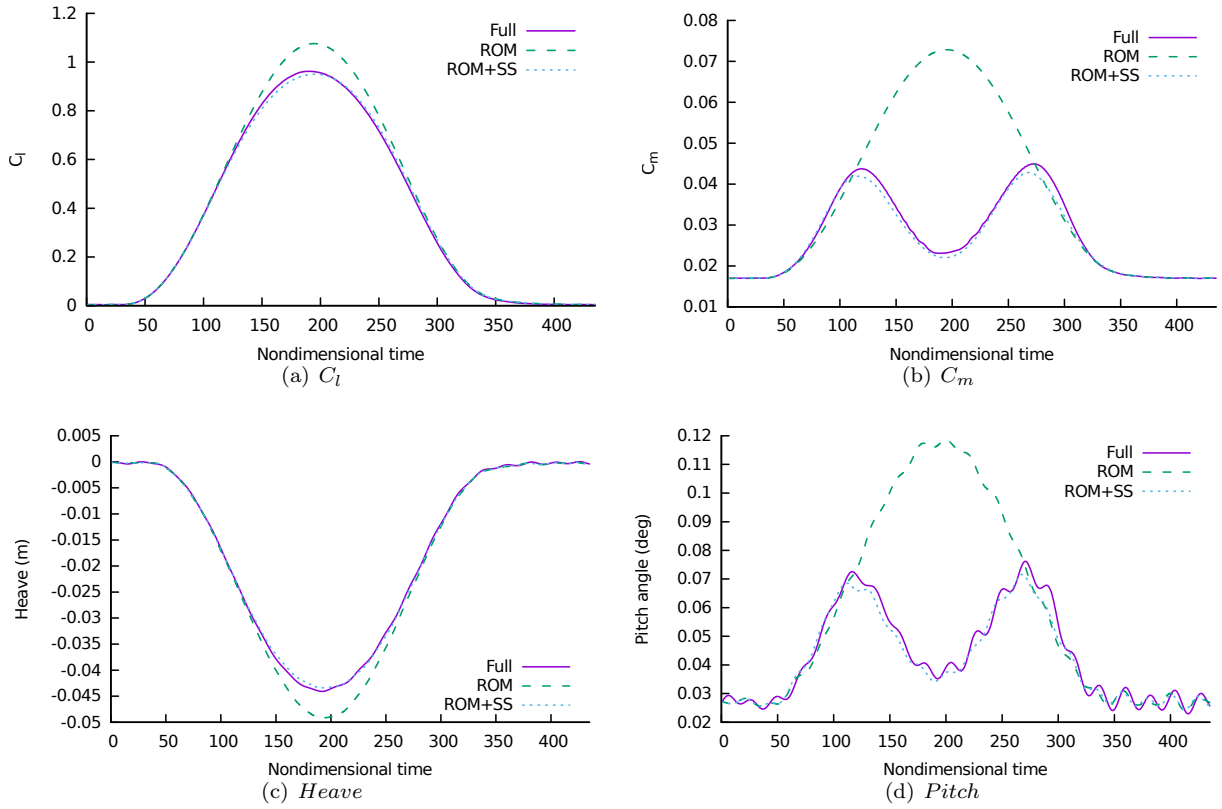

(a) C_l (b) C_m (c) $Heave$ (d) $Pitch$

Figure 15. Aeroelastic response of crank airfoil to gust profile 4

Figures 16 to 19. This shows that the corrected DLM now matches the linear ROM response very closely. The major difference is that the linear ROM matches the lag in recovery once the gust has passed. This is especially noticeably in the shortest gust shown in Figure 16.

The correction applied to the DLM is a linear correction so it cannot change the DLM to produce the double peaks seen in the CFD pitching moments. The correction for the ROM varies based on the instantaneous gust velocity allowing non-linear effects to be introduced. The responses to the gust predicted by the non-linear ROM is shown in Figures 16 to 19. It can be seen that the lift coefficient is well predicted by both the non-linear ROMs and the corrected DLM for all gust lengths. However for the moment the non-linear ROM gives much better agreement at all except the shortest gust length; this is similar to the 2D test cases given above. The linear ROM is better for the shorter gusts because the gust is not long enough for the shock to move as far and the correction applied is too large. Including the steady state data improves the predictive capability of the ROM because in the cases investigated the flow over the wing goes from being shock free to having a shock on the top surface at the peak gust velocities. The appearance of the shock is a non-linear behaviour which is not captured by the linear ROM, but is better captured by the inclusion of non-linearity via steady state data.

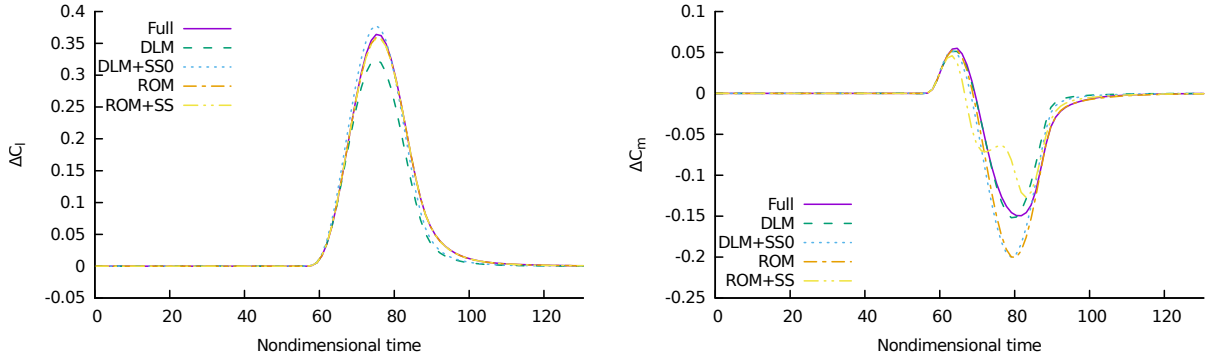

(a) C_l (b) C_m

Figure 16. Comparison of change in force coefficients of the FFAST wing predicted using non-linear ERA and corrected DLM with CFD, in response to gust case 1

Taking the moments about the leading edge of the wing root, gives the responses shown in Figure 21. Here the moment response is closer to linear as it is dominated by the lift component of the pitching moment. In this instance the linear ERA and the DLM, corrected close to alpha zero, give a good match to the moment. The linear ERA is closer to the CFD results while the corrected DLM over predicts the peak loads. Once again the linear ERA captures the lag in the pitching moment recovery, due to the shock motion, for case 1.

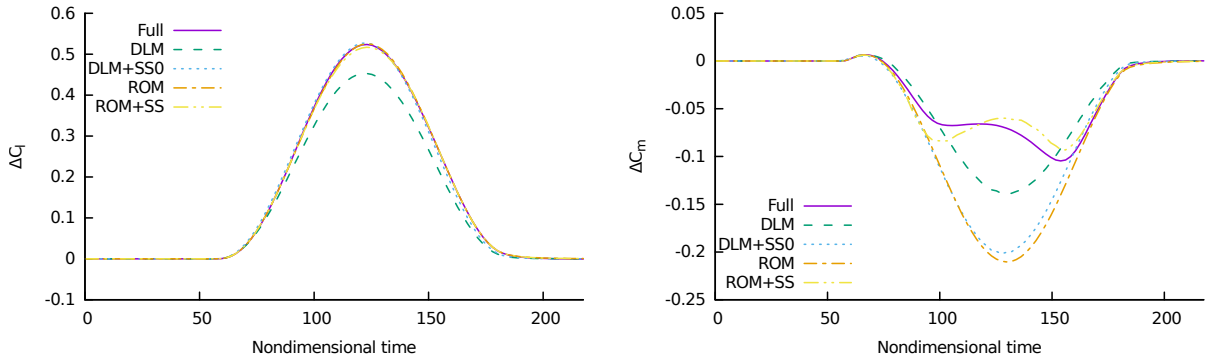

(a) C_l (b) C_m

Figure 17. Comparison of change in force coefficients of the FFAST wing predicted using non-linear ERA and corrected DLM with CFD, in response to gust case 2

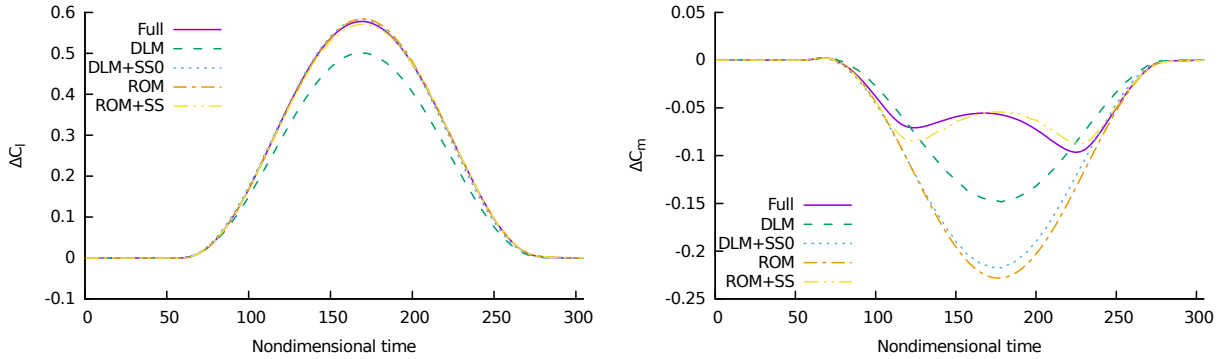

(a) C_l (b) C_m

Figure 18. Comparison of change in force coefficients of the FFAST wing predicted using non-linear ERA and corrected DLM with CFD, in response to gust case 3

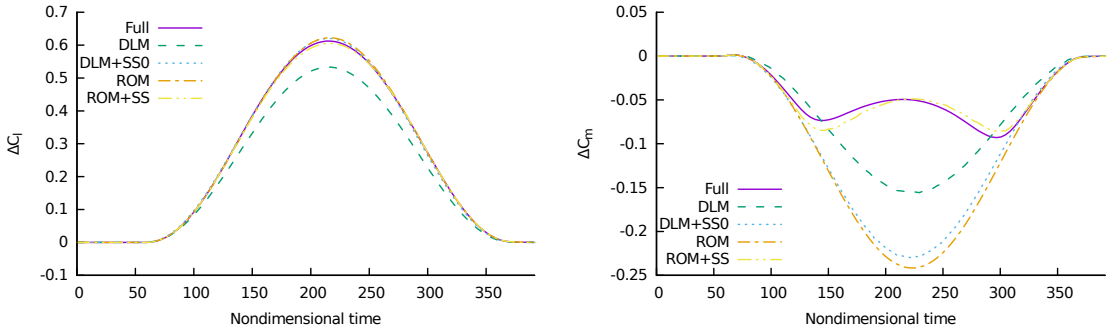

(a) C_l (b) C_m

Figure 19. Comparison of change in force coefficients of the FFAST wing predicted using non-linear ERA and corrected DLM with CFD, in response to gust case 4

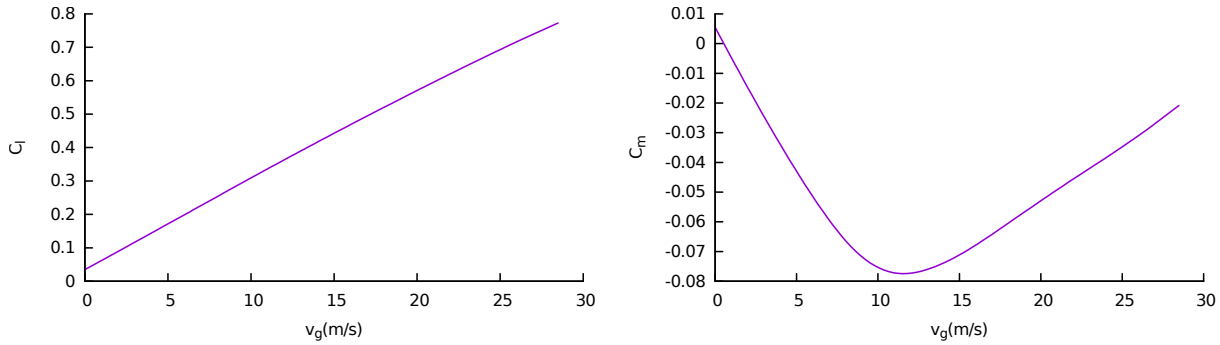

(a) C_l (b) C_m

Figure 20. Steady state lift and moment coefficient with gust velocity for FFAST wing

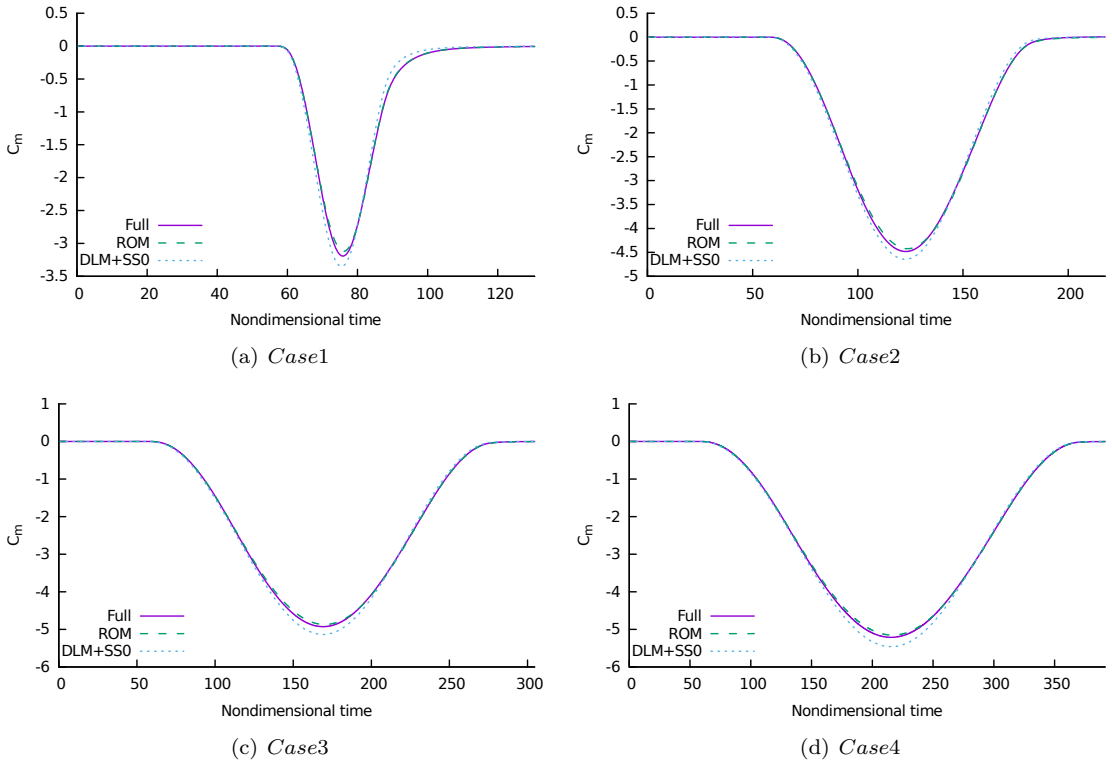

(a) $Case1$ (b) $Case2$

(c) $Case3$ (d) $Case4$

Figure 21. Comparison of change in moment coefficients for the FFAST wing predicted using linear ERA and corrected DLM with CFD, in response to different length gusts

A. Model size

For ROMs, accuracy generally increases as ROM size increases, however so does the cost of constructing and running the ROM. Thus there often needs to be a trade off between cost and accuracy. The impact of ROM size on the solution accuracy for the four gusts is shown in Figures 22 to 25. Each ROM was created from a Hankel matrix of size 500. For all cases the rank 5 model under predicts the full order results by the greatest amount and also does not quite capture the correct recovery after the peak gust response, particularly for the moment. The rank 10 model however does accurately model the gust recovery as well as being closer to matching the peak forces. Little further accuracy is gained by increasing the model size further to 20.

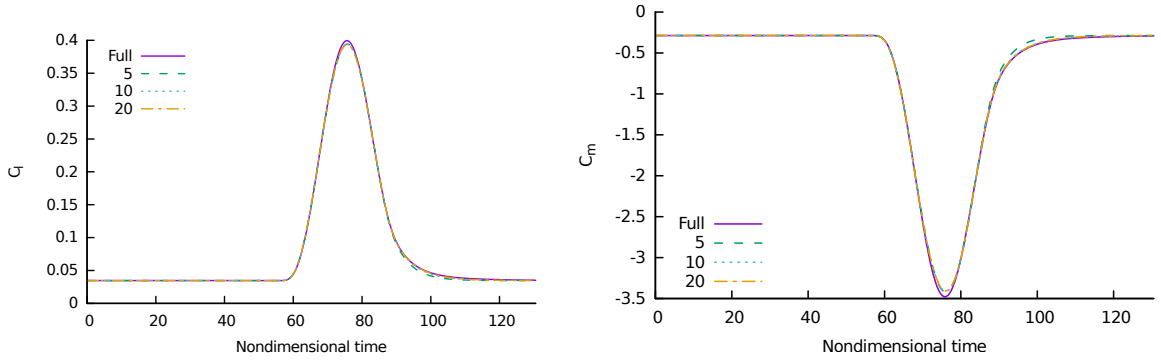

(a) C_l (b) C_m

Figure 22. Response of FFAST wing for varying ROM size: gust case 1

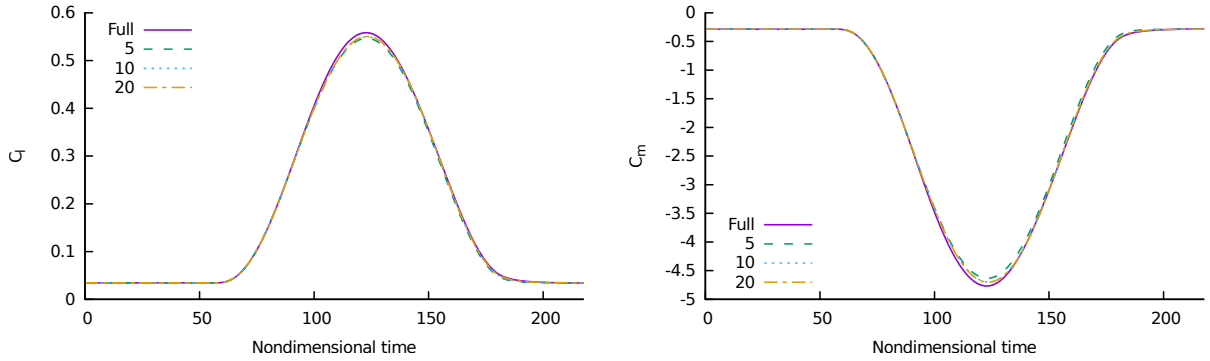

(a) C_l (b) C_m

Figure 23. Response of FFAST wing for varying ROM size: gust case 2

B. Number of Markov parameters

For a given size of model, the size of the Hankel matrix and thus the number of Markov parameter used, affects the accuracy of the resulting ROM. It might therefore appear to be advantageous to use a very large Hankel matrix for all ROM construction. However increasing the number of Markov parameters used is responsible for increasing the costs of construction. Also since the Markov parameters decrease in size using

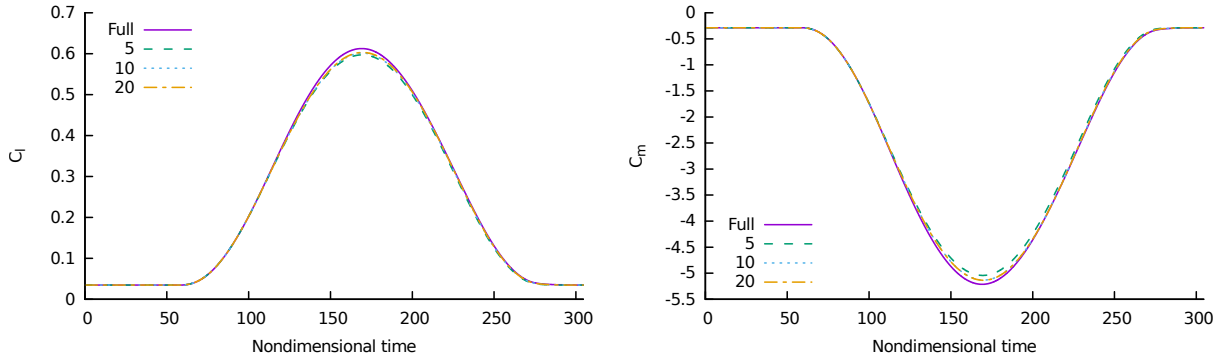

(a) C_l (b) C_m

Figure 24. Response of FFAST wing for varying ROM size: gust case 3

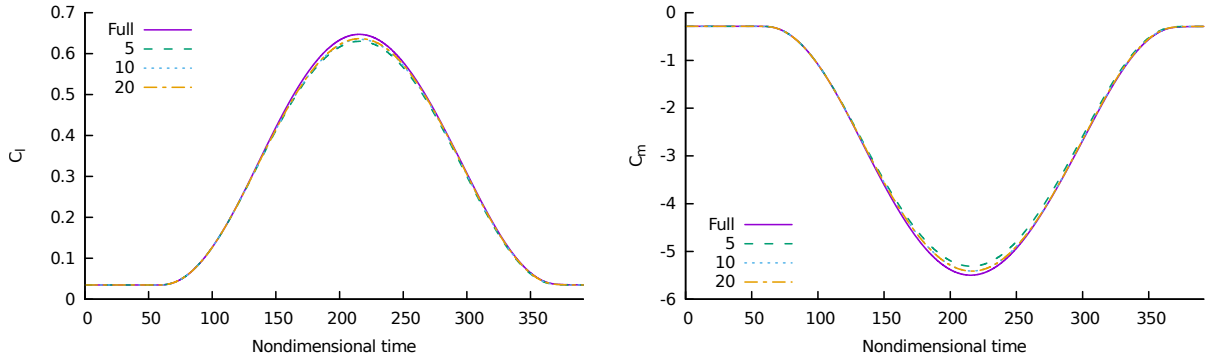

(a) C_l (b) C_m

Figure 25. Response of FFAST wing for varying ROM size: gust case 4

too many can lead to identification of numerical rather than physical modes which may reduce accuracy. For the case of a ROM for the FFAST wing of size 45, the minimum number of time steps needed to model the gust response without losing accuracy was investigated. Figures 26 to 29 show the effect of the size of the Hankel matrix on the response predicted by the ROM. This study shows that using a Hankel matrix of rank 100 leads to a model that does not match the gust recovery, predicting a slightly short response. Increasing the Hankel matrix size to 300 improves the predicted gust recovery time and prediction of the peak force. A Hankel matrix of rank 300 corresponds in this case to calculating the time history of the response until the step gust is 29 chords downstream of the wing. Further increasing the Hankel size does not yield any significant improvement in the accuracy of the predicted response, but increase the computational expense of creating the ROM.

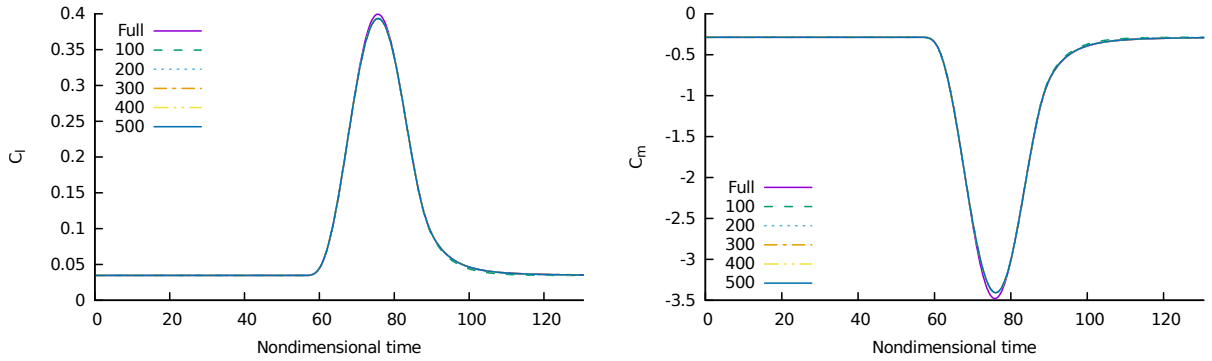

(a) C_l (b) C_m

Figure 26. Force coefficient history of FFAST wing in response to gust case 1, for ROMs constructed using different sized Hankel matrices

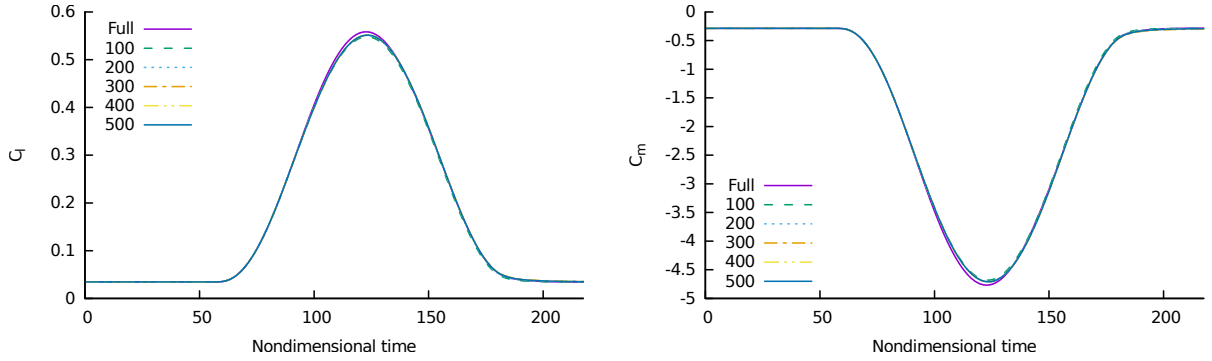

(a) C_l (b) C_m

Figure 27. Force coefficient history of FFAST wing in response to gust case 2, for ROMs constructed using different sized Hankel matrices

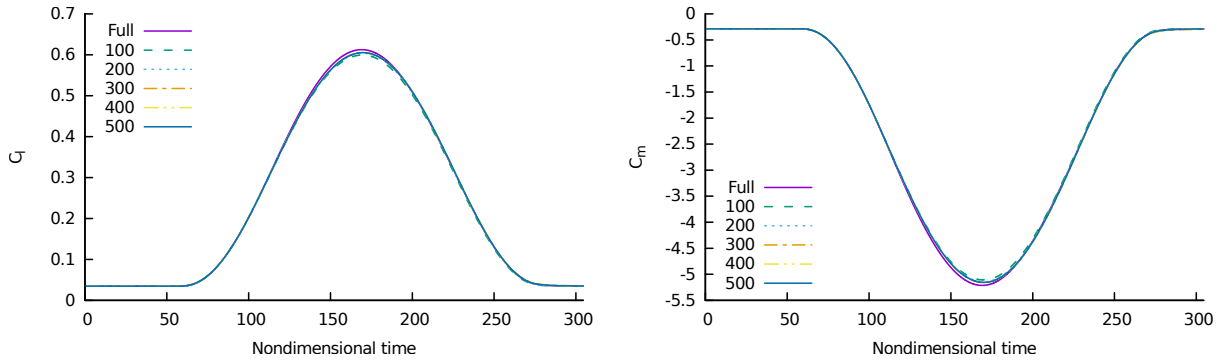

(a) C_l (b) C_m

Figure 28. Force coefficient history of FFAST wing in response to gust case 3, for ROMs constructed using different sized Hankel matrices

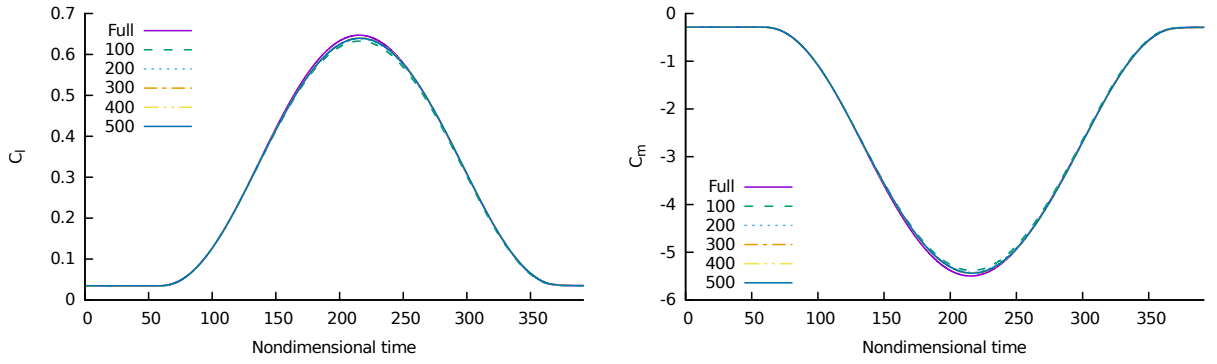

(a) C_l (b) C_m

Figure 29. Force coefficient history of FFAST wing in response to gust case 4, for ROMs constructed using different sized Hankel matrices

VII. Conclusions

This paper describes and presents results for two reduced order models for gust response prediction. The method for identifying the linear ROM requires the response to two sharp edged gust responses. Whilst such simulations are quite expensive, the ROM can be identified from a fairly short time history. Thus the cost of generating the ROM is less then calculating the response of even the shortest gust tested here. The resulting ROM is then of the order of 10s of unknowns, making it cheap to run multiple gust profiles and sizes at a given flight condition, representing a cost saving over carrying out all simulations with full order CFD.

Correcting the DLM to match the lift curve slope at the initial angle of attack gives a response close to the linear ROM, matching the lift well. However it over predicts the moment response to a gust, as does the linear ROM. The steady state moment about quarter mean aerodynamic chord is non-linear and the DLM results are sensitive to the choice of lift curve slope chosen to try and match the non-linear response.

Comparisons of the ROM models for four 1-cosine gust lengths shows that both the linear and non-linear ROMs give reasonable predictions at low gust lengths for the 2D and 3D, rigid and aeroelastic test cases considered. However at higher gust lengths the linear model accuracy reduces since there is a large shock motion. This is particularly apparent for the aeroelastic test cases. In contrast the non-linear method maintains a reasonable level of accuracy even as the gust length increases. The non-linear ROM results slightly under predict the peak pitch angle and pitching moment. This is in part due to the smaller pitching moment about the structural axis, compared to the leading edge, which means that the errors in the ROM due to the large shock motion result in a larger percentage error. However, any small errors have to be taken relative to the large non-linear shock motion in these cases. The inclusion of the steady state data in the model therefore can be used to improve the linear ROM at a relatively low additional computational cost.

Acknowledgements

The research leading to these results received funding from the European Communitys Seventh Framework Programme (FP7/2007-2013) under a grant agreement number 233665. FFAST (Future Fast Aeroelastic Simulation Technologies) is a collaborative research project aimed at developing, implementing and assessing a range of numerical simulation technologies to accelerate future aircraft design. Advances in critical load identification and reduced order modelling methods will potentially provide a step change in the efficiency and accuracy of the dynamic aeroelastic loads process. The partners in FFAST are: University of Bristol, INRIA, CSIR, TU Delft, DLR, IRIAS, University of Liverpool, Politecnico di Milano, NUMECA, Optimad Engineering, Airbus, EADS-Cassadian, IITP and UCT.

References

[1]J.R. Wright and J.E. Cooper. *Introduction to aircraft aeroelasticity and loads*. Wiley, 2007.

[2]G. Yang and S. Obayashi. Gust Response Analysis for SST with Navier-Stokes Equations. *Journal of Aircraft*, 41(6):1353–1359.

[3]L. Tang and J.D. Baeder. Adaptive Euler simulations of airfoil–vortex interaction. *International journal for numerical methods in fluids*, 53(5):777–792, 2007.

[4]J. Sitaraman. CFD Based Unsteady Aerodynamic Modeling For Rotor Aeroelastic Analysis. 2003.

[5]R. Singh and J. D. Baeder. Generalized Moving Gust Response Using CFD with Application to Airfoil-Vortex Interaction. *AIAA Paper*, pages 97–2208, 1997.

[6]A. Zaide and D. Raveh. Numerical simulation and reduced-order modeling of airfoil gust response. *AIAA journal*, 44(8):1826–1834, 2006.

[7]C. Wales, D. Jones, and A. Gaitonde. Simulation of airfoil gust responses using prescribed velocities. In *Proceedings IFASD 2011*, Paris, France, June 2011.

[8]M.C. Romanowski. Reduced order unsteady aerodynamic and aeroelastic models using karhunenloeve eigenmodes. In *Proceedings of the Sixth AIAA Symposium on Multidisciplinary Analysis and Optimization 1996, AIAA Paper 96-3981*, 1996.

[9]M.C. Romanowski and E.H. Dowell. Reduced order euler equations for unsteady aerodynamic flows: numerical techniques. *AIAA Paper*, 96-0528, 1996.

[10]K.C. Hall, J.P. Thomas, and E.H. Dowell. Proper orthogonal decomposition technique for transonic unsteady aerodynamic flows. *AIAA Journal*, 38(10):1853–1862, 2000.

[11]Karen Willcox and Jaime Peraire. Balanced model reduction via the proper orthogonal decomposition. *AIAA journal*, 40(11):2323–2330, 2002.

[12]D.E. Raveh. Reduced-order models for nonlinear unsteady aerodynamics. *AIAA Journal*, 39(8):1417–1429, 2001.

[13]W.A. Silva. *Discrete-Time Linear and Nonlinear Aerodynamic Impulse Responses for Efficient CFD Analyses*. PhD thesis, Department of Applied Science, College of William and Mary, Virginia, USA, 1997.

[14]A.L. Gaitonde and D.P. Jones. A two-dimensional linearized unsteady Euler scheme for pulse response calculations. *Proceedings of the Institution of Mechanical Engineers, Part G: Journal of Aerospace Engineering*, 216(2):89–104, 2002.

[15]J.N. Juang and R.S. Pappa. Eigensystem realization algorithm for modal parameter identification and model reduction. *Journal of Guidance, Control, and Dynamics*, 8(5):620–627, 1985.

[16]Z. Ma, S. Ahuja, and C. Rowley. Reduced order models for control of fluids using the eigensystem realization algorithm. *Theor. Comput. Fluid Dyn.*, 25:233–247, 2011.

[17]C. Wales, D. Jones, and A. Gaitonde. Prescribed Velocity Method for Simulation of Aerofoil Gust Responses. *Journal of Aircraft*, 52:64–76, 2015.

[18]A.L. Gaitonde and D.P. Jones. Study of linear response identification techniques and reduced-order model generation for a 2D CFD scheme. *International Journal for Numerical Methods in Fluids*, 52(12):1361–1402, 2006.

[19]T. Gerhold, O. Friedrich, J. Evans, and M. Galle. Calculation of complex three-dimensional configurations employing the DLR-TAU-code. *AIAA Paper*, (97-0167), 1997.

[20]M. Galle, T. Gerhold, and J. Evans. Parallel computation of turbulent flows around complex geometries on hybrid grids with the dlr-tau code. In A. Ecer and D. R. Emerson, editors, *Proc. 11th Parallel CFD Conference*, May 1999.

[21]C. Wales, D. Jones, and A. Gaitonde. Reduced Order Modelling for Aeroelastic Aerofoil Response to a Gust. *AIAA Paper 2013-0790*, 2013.

[22]D. Jones and A. Gaitonde. Future fast methods for loads calculations: The FFAST project. In *Proceedings Aerodays 2011*, Madrid, Spain, 2011.

[23]C Wales, A Gaitonde, and D Jones. Stabilisation of reduced order models via restarting. *International Journal for Numerical Methods in Fluids*, 73(6):578–599, 2013.

[24]J.P Giesing, T.P Kalman, and W.P Rodden. Correction factor techniques for improving aerodynamic prediction methods. 1976.